

# Oxygen superstructures throughout the phase diagram of $(Y, Ca)Ba_2Cu_3O_{6+x}$

J. Strempfer<sup>1</sup>, I. Zegkinoglou<sup>1</sup>, U. Rütt<sup>1</sup>, M. v. Zimmermann<sup>2</sup>, C. Bernhard<sup>1</sup>, C. T. Lin<sup>1</sup>, Th. Wolf<sup>3</sup>, and B. Keimer<sup>1</sup>

<sup>1</sup> *Max-Planck-Institut für Festkörperforschung, Heisenbergstr. 1, D-70569 Stuttgart, Germany*

<sup>2</sup> *Hamburger Synchrotronstrahlungslabor HASYLAB at Deutsches*

*Elektronen-Synchrotron DESY, Notkestr. 85, D-22603 Hamburg, Germany and*

<sup>3</sup> *Forschungszentrum Karlsruhe, IFP, D-76021 Karlsruhe, Germany*

(Dated: June 17, 2018)

Short-range lattice superstructures have been studied with high-energy x-ray diffuse scattering in underdoped, optimally doped, and overdoped  $(Y, Ca)Ba_2Cu_3O_{6+x}$ . A new four-unit-cell superstructure was observed in compounds with  $x \sim 0.95$ . Its temperature, doping, and material dependence was used to attribute its origin to short-range oxygen vacancy ordering, rather than electronic instabilities in the  $CuO_2$  layers. No significant diffuse scattering is observed in  $YBa_2Cu_4O_8$ . The oxygen superstructures must be taken into account when interpreting spectral anomalies in  $(Y, Ca)Ba_2Cu_3O_{6+x}$ .

PACS numbers: 74.72.Bk, 61.10.Eq

The two-dimensional strongly correlated electron system in the layered copper oxides is known to be susceptible to at least two types of instabilities at nonzero doping: high temperature superconductivity, and “stripe” ordering of spin and charge degrees of freedom [1]. The question of whether fluctuating stripes are a prerequisite for high temperature superconductivity remains one of the central unanswered questions in the field. Several experimental techniques are suitable as probes of stripe order and fluctuations, including x-ray scattering, magnetic and nuclear neutron scattering, NMR and NQR, and scanning tunneling spectroscopy [1]. X-rays couple directly to the charge, and the high photon energy ensures that both static charge ordering and charge excitations up to high energies can be detected. Notably, x-ray superstructure reflections due to static stripe ordering were observed in Nd-substituted  $La_{2-x}Sr_xCuO_4$  [2] following an initial observation by neutron diffraction [3]. Furthermore, a recent x-ray scattering study of underdoped  $YBa_2Cu_3O_{6+x}$  has uncovered diffuse features whose temperature dependence was reported to exhibit an anomaly around the “pseudogap” temperature [4]. This anomaly was interpreted as a signature of electronic stripe formation. In this system, however, superstructures due to oxygen ordering with wave vectors depending sensitively on the oxygen content are also observed [5]. As both phenomena are associated with lattice distortions and are thus expected to be intimately coupled, it is difficult to establish which features of the x-ray data originate in short range oxygen ordering, and which can be attributed to electronic stripe ordering or fluctuations.

In order to answer this question unambiguously, we have investigated the x-ray diffuse intensity in underdoped, optimally doped, and overdoped  $(Y, Ca)Ba_2Cu_3O_{6+x}$  single crystals. Surprisingly, diffuse features with a well defined four-unit-cell periodicity were observed even in optimally doped  $YBa_2Cu_3O_{6.92}$  where the density of oxygen vacancies is low. However, the dif-

fuse features were observed to depend only on the oxygen concentration  $x$  in  $YBa_2Cu_3O_{6+x}$  and not on the charge carrier concentration in the  $CuO_2$  planes which was varied independently from the oxygen content through Ca substitution. In addition, no significant diffuse scattering was observed in  $YBa_2Cu_4O_8$ , a naturally underdoped material that does not sustain oxygen defects. The diffuse intensity therefore arises from short-range oxygen ordering and associated lattice distortions, and any signatures of stripe ordering or fluctuations must be much weaker. The oxygen superstructure induces substantial lattice deformations in the  $CuO_2$  layers and must be taken into account when interpreting phonon anomalies in this material [6, 7].

The experiments were conducted at the high-energy wiggler beamlines BW5 at the Hamburger Synchrotronstrahlungslabor at the Deutsches Elektronen-Synchrotron and 11-ID-C at the Advanced Photon Source at the Argonne National Laboratory. The x-ray energies were 100 keV and 115 keV, respectively. Both beamlines were optimized for providing as much flux as possible for the broad diffuse reflections. This was achieved by using a broad energy bandwidth. At 11-ID-C, a Si-(3,1,1) monochromator is located almost at the 1:1 position between beam source (wiggler) and sample position. Therefore, the entire 10 mm width of the Laue monochromator crystal can be used for focusing on the sample [8]. At BW5, a Si-Ge-gradient crystal diffracting a large energy bandwidth due to the lattice parameter variation was used as monochromator [9].

The samples studied included one optimally doped  $YBa_2Cu_3O_{6+x}$  crystal with  $x \sim 0.92$  and  $T_c = 92.7$  K, two underdoped  $YBa_2Cu_3O_{6+x}$  crystals with  $x \sim 0.75$  and  $T_c = 67$  K and  $x \sim 0.65$  and  $T_c = 60$  K, respectively, and a highly overdoped crystal of composition  $Y_{0.8}Ca_{0.2}Ba_2Cu_3O_{6.95}$  and  $T_c = 73$  K [10]. The crystal volumes were approximately  $2 \times 2 \times 0.4$  mm<sup>3</sup>, and the optimally and overdoped crystals were fully detwinned. In

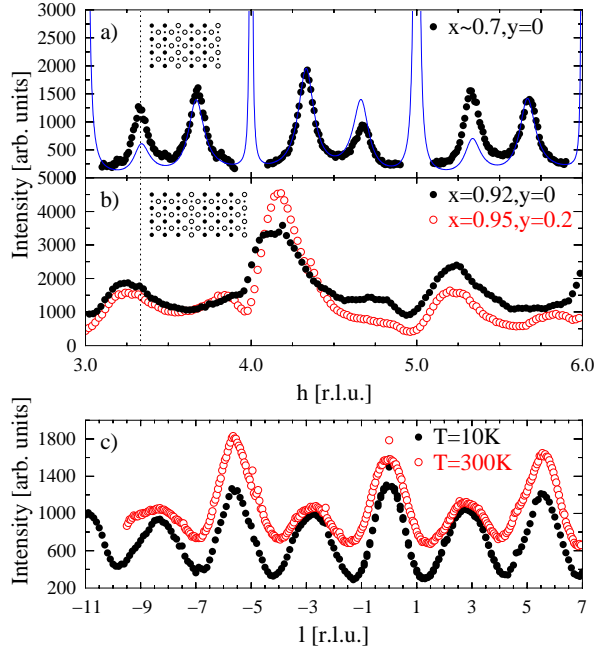


FIG. 1: Diffuse scattering intensities in  $Y_{1-y}Ca_yBa_2Cu_3O_{6+x}$ . (a) Scans along  $(h, 0, 2.5)$  for the ortho-III phase of  $YBa_2Cu_3O_{6.75}$ , together with a simulation (solid line) based on the structure found by Plakhty et al. [11]. (b)  $(h, 0, 5.6)$  scan for both  $YBa_2Cu_3O_{6.92}$  (●) and  $Y_{0.8}Ca_{0.2}Ba_2Cu_3O_{6.95}$  (○). (c)  $l$ -scans of  $YBa_2Cu_3O_{6.92}$  at both  $T=10K$  and  $T=300K$  along  $(4.25, 0, l)$ . The insets in a) and b) show the ortho-III and ortho-IV patterns, respectively, where large full (open) circles denote occupied (unoccupied) oxygen-sites.

addition, one untwinned  $YBa_2Cu_4O_8$  crystal of approximate volume  $0.5 \times 0.8 \times 0.1 \text{ mm}^3$  and  $T_c = 81 \text{ K}$  was investigated. In the following, the wave vector components  $(h, k, l)$  are indexed in the orthorhombic space group  $Pmmm$  for  $YBa_2Cu_3O_{6+x}$  and  $Ammm$  for  $YBa_2Cu_4O_8$ . The lattice parameters are  $a=3.8158(1)\text{\AA}$ ,  $b=3.8822(1)\text{\AA}$ , and  $c=11.6737(3)\text{\AA}$  for  $YBa_2Cu_3O_{6.92}$  at  $T = 270 \text{ K}$  and  $a=3.8410(3)\text{\AA}$ ,  $b=3.8720(3)\text{\AA}$  and  $c=27.231(2)\text{\AA}$  for  $YBa_2Cu_4O_8$ . The samples were mounted in closed-cycle cryostats capable of reaching temperatures between 10 and 300 K or between 20 and 500 K, depending on the experiment. The cryostats were mounted on four-circle goniometers to allow a wide coverage of reciprocal space. Due to the high photon energy, the x-ray penetration depth is comparable to the sample dimensions. Strain effects in the near-surface region, which can influence x-ray scattering measurements with lower photon energies, are thus not relevant here.

Fig. 1 shows the intensities of x-rays scattered from the underdoped, optimally doped and overdoped  $(Y, Ca)Ba_2Cu_3O_{6+x}$  single crystals described above. The

diffuse features shown are  $\sim 5$  orders of magnitude weaker than the main Bragg reflections. The intensity is peaked at wave vectors  $h = 0.33$  for  $YBa_2Cu_3O_{6.75}$ , and  $h = 0.25$  for  $YBa_2Cu_3O_{6.92}$  and  $Y_{0.8}Ca_{0.2}Ba_2Cu_3O_{6.95}$  (Figs. 1a-b), indicating short-range superstructures with periodicities equal to three and four elementary orthorhombic unit cells, respectively. As a function of the wave vector component  $l$  perpendicular to the copper oxide layers (Fig. 1c), the intensity shows a modulation with a periodicity characteristic of interatomic distances within the unit cell, in particular the distances between the copper oxide chain and plane layers and between the chain layer and the apical oxygen, as described in [4]. The diffuse scattering thus results from lattice displacements encompassing the entire unit cell.

While the four-cell superstructure in optimally and overdoped  $(Y, Ca)Ba_2Cu_3O_{6+x}$  has thus far not been reported, the three-cell superstructure in underdoped  $YBa_2Cu_3O_{6.75}$  is known as the “ortho-III phase” [5]. Its primary origin is an ordering of oxygen defects in a pattern in which one empty CuO chain follows two fully occupied chains (inset in Fig. 1a). Due to the oxygen diffusion kinetics, the ortho-III phase is always short-range ordered, and the width of the superlattice reflection of  $\Delta h = 0.12(1)$  r.l.u. we observe compares favorably with prior work [5, 11]. The measured intensities are also in good agreement with the literature, although some deviations are found (Fig. 1a). In particular, the intensity difference of the satellites with wave vectors  $\pm 0.33$  surrounding the main Bragg reflections is well reproduced by a calculation based on the atomic displacements given in Ref. [11]. Similar observations were made on the “ortho-V phase” of the  $YBa_2Cu_3O_{6.65}$  crystal (not shown).

We now turn to the newly discovered four-cell superstructures in optimally doped  $YBa_2Cu_3O_{6.92}$  and highly overdoped  $Y_{0.8}Ca_{0.2}Ba_2Cu_3O_{6.95}$ . The periodicities, intensities and correlation lengths of the superstructures in both samples are virtually identical within the statistical accuracy of the data. (The range around the  $(4, 0, 0)$  position in Fig. 1b has to be disregarded, because a tail of the main Bragg reflection obstructs the diffuse intensity.) Charge density wave or stripe correlations are expected to be characterized by a wave vector that depends strongly on the charge carrier concentration, and by an amplitude that is strongly reduced in heavily overdoped samples. As the charge carrier concentration in the  $CuO_2$  layers is very different in the two samples (whereas their oxygen content is nearly identical), we conclude that charge order or fluctuations within the layers can at most give a minor contribution to the diffuse intensity.

In analogy to the underdoped samples discussed above, we hence attribute the diffuse features in  $(Y, Ca)Ba_2Cu_3O_{6+x}$  samples with  $x \sim 0.95$  to an “ortho-IV” oxygen-ordered phase characterized, on average, by a sequence of three full and one empty CuO chain (inset in

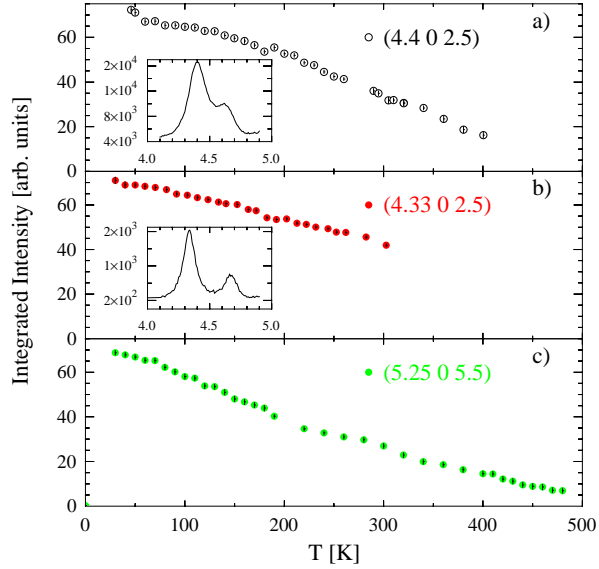


FIG. 2: Temperature dependences of the integrated intensity of (a) the  $(4.4, 0, 2.5)/(4.6, 0, 2.5)$  reflections in  $\text{YBa}_2\text{Cu}_3\text{O}_{6.65}$ , (b) the  $(4.33, 0, 2.5)/(4.66, 0, 2.5)$  reflections in  $\text{YBa}_2\text{Cu}_3\text{O}_{6.75}$  and the  $(5.25, 0, 5.6)$  reflections in  $\text{YBa}_2\text{Cu}_3\text{O}_{6.92}$ . The insets in (a) and (b) show the respective Q-scan at low temperature.

Fig. 1b). Because of the low density of oxygen defects, islands of the ortho-IV phase are expected to be small and dilute. This explains the large width of the superstructure peaks of  $\Delta h = 0.29(1)$  r.l.u. in this compound. A complementary way of looking at these data is through an analysis in terms of pair correlations between oxygen defects, which leads to a Fourier series for the diffuse intensity [12]. In fact, a single Fourier component corresponding to an enhanced probability for occupation of oxygen defects on third-nearest-neighbor chains already provides a good description of the width of the diffuse features in the  $(h, 0, 0)$  direction:  $I(h) \sim 1 - \alpha \cos(4\pi h)$ . This confirms the short range nature of the oxygen ordering. A quantitative description of the correlation coefficient  $\alpha$  in different Brillouin zones will require a more comprehensive simulation of the lattice distortions, which is beyond the scope of this paper. The salient features of the diffuse intensity, including especially the intensity asymmetry of the satellite features above and below the main Bragg reflections (Fig. 1b), are, however, similar to those observed in the ortho-III ordered sample, which implies similar atomic displacements.

The temperature dependences of the integrated intensities of the ortho-V, ortho-III and ortho-IV peaks are

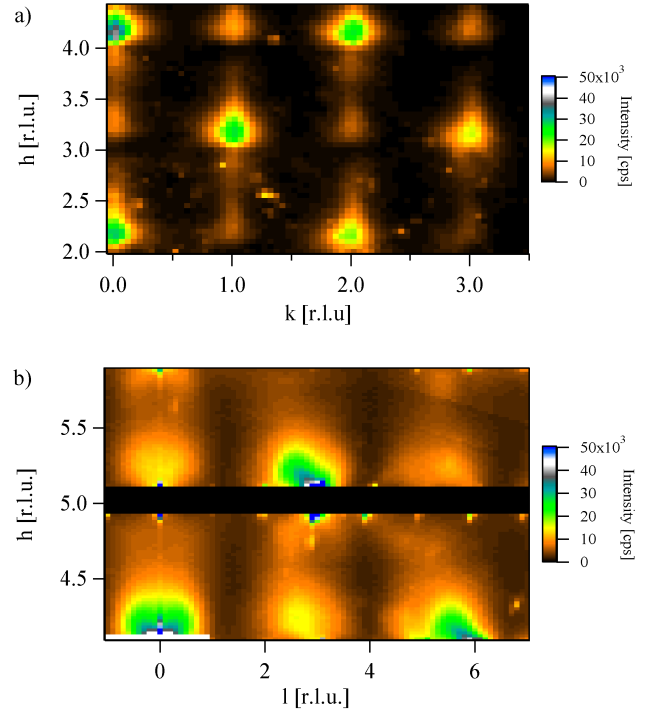


FIG. 3: Contour plots of the diffuse intensity in the (a)  $(h, k, 5.5)$ -plane and (b)  $(h, 0, l)$ -plane of  $\text{Y}_{0.8}\text{Ca}_{0.2}\text{Ba}_2\text{Cu}_3\text{O}_{6.95}$ . The main Bragg reflections are masked.

shown in Figs. 2a-c. Whereas for the ortho-V and ortho-III samples scans along  $h$  were performed, as shown in the insets, the integrated intensity of the optimally doped sample was obtained from  $l$ -scans over the diffuse peaks, as shown in Fig. 1c. This allows the most reliable subtraction of the temperature dependent background from thermal diffuse scattering. These temperature dependences further confirm that all features originate in oxygen ordering rather than charge instabilities in the  $\text{CuO}_2$  layers. Independent of the doping level, the superstructures persist well above room temperature, with no anomalies observed at the superconducting transition temperature or other temperatures associated with the onset of electronic instabilities. In particular, our data are at variance with Islam *et al.*'s claim of an anomalous temperature dependence of the ortho-V reflections near the onset of the electronic “pseudogap” [4]. The intensity variation observed in Ref. [4] is clearly outside the statistical variation of the data of Fig. 2a. Rather, the intensity of the diffuse features is reduced smoothly upon heating and vanishes around 400-450 K. Prior work in samples with  $0.5 \leq x \leq 0.8$  has shown that in this temperature range, oxygen order is obliterated due to progressively rapid oxygen diffusion [5].

Fig. 3 shows maps of the diffuse intensity in the  $(h, k, 5.5)$  and  $(h, 0, l)$  scattering planes for the  $\text{Y}_{0.8}\text{Ca}_{0.2}\text{Ba}_2\text{Cu}_3\text{O}_{6.95}$  sample. Similar maps for the

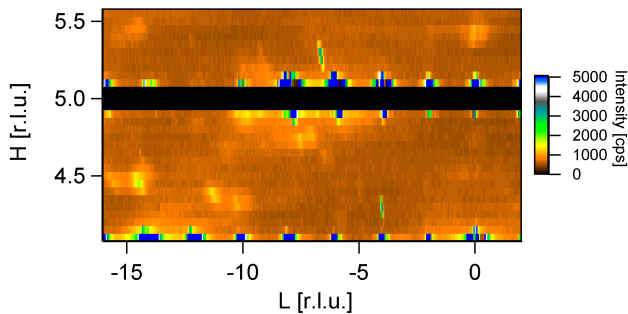


FIG. 4: Contour plot of the diffuse intensity in the  $(h, 0, l)$  scattering plane of  $\text{YBa}_2\text{Cu}_4\text{O}_8$ .

$\text{YBa}_2\text{Cu}_3\text{O}_{6.92}$  sample (not shown) are nearly indistinguishable from those of Fig. 3, in accord with Fig. 1b. Panel a shows that the superstructure is only observed along the  $a$ -direction, that is, perpendicular to the  $\text{CuO}$  chains. Diffuse features induced by charge density wave ordering along the chains are not observed above background. X-ray signatures of electronic instabilities both in the chains and in the layers must therefore be much weaker than the manifestations of the short-range oxygen vacancy order we observe.

This conclusion is underscored by an intensity map of  $\text{YBa}_2\text{Cu}_4\text{O}_8$ , shown in Fig. 4 on the same scale as those of Fig. 3. Since this material does not sustain oxygen defects, diffuse scattering due to stripe or charge density wave ordering should be much more easily visible than in  $\text{YBa}_2\text{Cu}_3\text{O}_{6+x}$ . However, no such intensity is observed at least down to the intensity level of the diffuse peaks in the optimally doped compound.

Finally, prompted by reports of large isotope effects on various physical properties of high temperature superconductors [13], we have also investigated an optimally doped  $\text{YBa}_2\text{Cu}_3\text{O}_{6.92}$  crystal in which  $^{16}\text{O}$  was completely exchanged by  $^{18}\text{O}$ . The diffuse scattering pattern (not shown) was found to be virtually identical to that of the  $^{16}\text{O}$ -rich material. This excludes variations in oxygen short-range order as the origin of the observed isotope effects, at least for the  $\text{YBa}_2\text{Cu}_3\text{O}_{6+x}$  system.

In conclusion, we have observed a superstructure with a four-unit-cell periodicity in  $(\text{Y}, \text{Ca})\text{Ba}_2\text{Cu}_3\text{O}_{6+x}$  materials with  $x \sim 0.95$ . The superstructure involves atomic displacements throughout the unit cell, but its origin can unambiguously be attributed to a short-range ordering of oxygen vacancies. This is supported by three independent observations: the similarity of the diffuse scattering patterns of the  $\text{YBa}_2\text{Cu}_3\text{O}_{6.92}$  and  $\text{Y}_{0.8}\text{Ca}_{0.2}\text{Ba}_2\text{Cu}_3\text{O}_{6.95}$  compounds, which have similar oxygen content but different charge carrier concentrations; the absence of diffuse reflections in the scattering pattern of the  $\text{YBa}_2\text{Cu}_4\text{O}_8$  compound, which contains no oxygen vacancies; and the persistence of the diffuse intensities up to temperatures well above room temperature.

Charge density modulations along the  $\text{CuO}$  chains of  $\text{YBa}_2\text{Cu}_3\text{O}_{6+x}$  have been addressed both in the experimental [14, 15, 16, 17] and in the theoretical [18] literature. Experimental evidence includes variations of the NQR frequencies of both chain and plane  $^{63}\text{Cu}$  nuclei, as well as spatially periodic modulations of the tunnelling conductance in STM studies. These observations have been interpreted in terms of either charge density wave correlations [14, 15, 16] or Friedel-type oscillations around oxygen defects in the chains [17, 18]. Subtle modulations of the valence electron density along the chains may be too weak to be observed by x-rays in the presence of much stronger diffuse scattering from short-range ordered oxygen defects (which involves all core electrons). However, our observation of significant interchain correlations in the positions of oxygen defects may lead to a more quantitative understanding of the NQR and STM results. Indeed, correlations between charge density modulations on different chains observed in STM images [17] may well originate in the correlations between oxygen vacancies reported here.

As an integral part of the lattice structure of optimally doped  $\text{YBa}_2\text{Cu}_3\text{O}_{6+x}$ , probably the most extensively investigated high temperature superconductor – stoichiometric  $\text{YBa}_2\text{Cu}_3\text{O}_7$  is overdoped and difficult to prepare – the oxygen ordering-induced superstructure may also be relevant for the interpretation of a variety of other spectral features. In particular, this component of the real lattice structure should be taken into account when interpreting phonon anomalies in underdoped [6] and optimally doped [7]  $\text{YBa}_2\text{Cu}_3\text{O}_{6+x}$ , which are expected to be sensitive to the local lattice displacements reported here. Finally, based on our findings we suggest to investigate short-range correlations between oxygen defects and their potential impact on spectroscopic features in other families of high temperature superconductors as well.

We thank B. Dabrowski (NIU) for providing the  $\text{YBa}_2\text{Cu}_4\text{O}_8$  sample and J.C. Davis, S.C. Moss, and P. Wochner for valuable discussions. Use of the Advanced Photon Source is supported by the U.S. Department of Energy, Office of Science, Office of Basic Energy Sciences, under contract W-31-109-Eng-38.

- 
- [1] For a review, see S.A. Kivelson *et al.*, cond-mat/0210683.
  - [2] M. v. Zimmermann *et al.*, Europhys. Lett. **41**, 629 (1998).
  - [3] J. M. Tranquada *et al.*, Nature **375**, 561 (1995); Phys. Rev. B **54**, 7489 (1996)..
  - [4] Z. Islam *et al.*, Phys. Rev. B **66**, 092501 (2002).
  - [5] N. H. Andersen *et al.*, Physica C **317-318**, 259 (1999).
  - [6] H. A. Mook *et al.*, Nature **395**, 580 (1998); H. A. Mook and F. Dogan, Nature **401**, 145 (1999).
  - [7] L. Pintschovius *et al.*, cond-mat/0308357.
  - [8] U. Rütt *et al.*, Nucl. Instrum. Methods A **467-468**, 1026 (2001).

- [9] S. Keitel *et al.*, Nucl. Instrum. Methods A **414**, 427 (1998).
- [10] T. Zenner *et al.*, J. Low Temp. Phys. **105**, 909 (1996); C. T. Lin, B. Liang, and H. C. Chen, J. Cryst. Growth **237-239**, 778 (2002).
- [11] V. Plakhty, P. Burlet, and J. Y. Henry, Phys. Lett. A **198**, 256 (1995).
- [12] J. M. Cowley, J. Appl. Phys. **21**, 24 (1950).
- [13] See, *e.g.*, D.R. Temprano *et al.*, Phys. Rev. Lett. **84**, 1990 (2000); C. Bernhard *et al.*, cond-mat/0306097.
- [14] S. Krämer and M. Mehring, Phys. Rev. Lett. **83**, 396 (1999).
- [15] B. Grevin, Y. Berthier, and G. Collin, Phys. Rev. Lett. **85**, 1310 (2000).
- [16] M. Maki *et al.*, Phys. Rev. B **65**, 140511 (2002).
- [17] D.J. Derro *et al.*, Phys. Rev. Lett. **88**, 097002 (2002); J.C. Davis (private communication).
- [18] D.K. Morr and A.V. Balatsky, Phys. Rev. Lett. **87**, 247002 (2001); *ibid.* **90**, 067005 (2003).